ChemComm

Selective heterogeneous capture and release of actinides using carborane-functionalized electrodes

Journal:	*ChemComm*
Manuscript ID	CC-COM-05-2023-002135.R1
Article Type:	Communication

COMMUNICATION

Selective heterogeneous capture and release of actinides using carborane-functionalized electrodes

Maxwell Mattejat[a] and Gabriel Ménard*[a,b]

Received 00th January 20xx,
Accepted 00th January 20xx

DOI: 10.1039/x0xx00000x

We report the heterogenization of molecular, electrochemically switchable *ortho*-substituted carboranes (^{PO}Cb, ^{PO}Cb-Pyr) for selective metal capture. Films of ^{PO}Cb and ^{PO}Cb-Pyr on glassy carbon and carbon fiber (CF) electrodes demonstrated heterogeneous electrochemical behaviour that was enhanced by the inclusion of single-walled carbon nanotubes (CNTs). Galvanostatically charged CF|CNT|^{PO}Cb and CF|CNT|^{PO}Cb-Pyr electrodes selectively captured and released actinides (Th^{4+}, UO_2^{2+}) from a mixed solutions containing alkali (Cs^+), lanthanide (Nd^{3+}, Sm^{3+}) and actinide (Th^{4+}, UO_2^{2+}) metal ions.

Nuclear power plays a key role in the rapid decarbonization of our global energy grid. Globally 443 reactors are currently operational, with 52 more under construction, in total generating 11% of global electricity.[1] The uranium that constitutes the bulk (~ 95%) of generated spent nuclear fuel (SNF) from these reactors can potentially be recycled, but must be separated from the SNF components which includes Pu, minor actinides, lanthanides, Tc, Mo, I, Cs, and others.[2] The main separation process – the Plutonium Uranium Redox EXtraction (PUREX) process – isolates clean streams of uranyl (UO_2^{2+}) and Pu^{3+} from all other radionuclides using a biphasic liquid-liquid extraction method.[3] The generation of pure streams of Pu, however, is a major concern for nuclear weapons proliferation.[3] A further drawback is the reliance on organic solvents (e.g., kerosene) and the subsequent generation of high volumes of radioactive waste – an issue that could be addressed via heterogeneous separation processes.

We have previously reported an electrochemical analog of the PUREX process utilizing an *ortho*-substituted *nido*-carborane anion, $[1,2\text{-}(Ph_2PO)_2\text{-}1,2\text{-}C_2B_{10}H_{10}]^{2-}$ ($^{PO}Cb^{2-}$) to selectively capture uranyl (UO_2^{2+}) from simulated SNF (Cs^+, Nd^{3+}, Sm^{3+}, UO_2^{2+}, Th^{4+} (used as a Pu^{4+} surrogate)) (Fig. 1a).[4, 5] This generated a "captured" uranyl species, $[UO_2(^{PO}Cb)_2]^{2-}$, in the dichloroethane (DCE) organic layer, which was subsequently electrochemically oxidized back to the *closo*-carborane (^{PO}Cb) species releasing the UO_2^{2+}. The released UO_2^{2+} was then back extracted into a fresh aqueous solution.

In this work, we describe the heterogenization of our molecular carborane species onto an electrode surface to target the selective heterogenous capture and release of actinides vs.

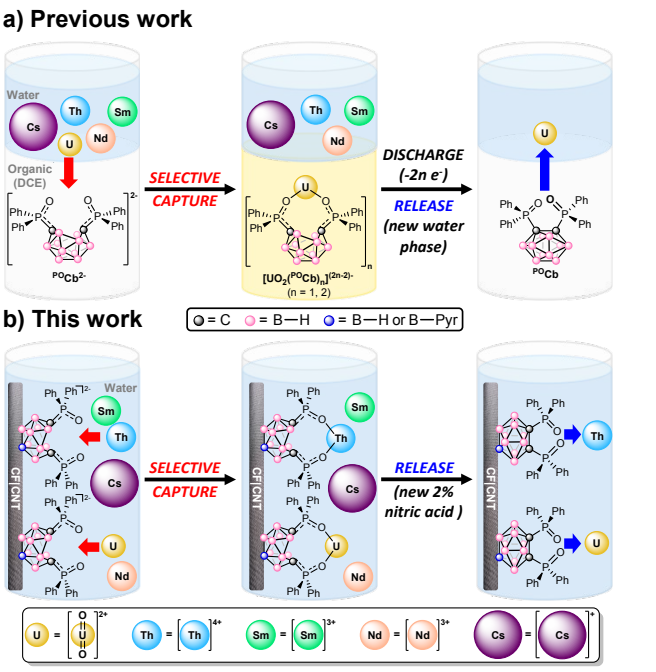

Fig. 1 a) Our previous work on selective uranyl capture and release using an electrochemical biphasic scheme. b) This work highlighting heterogeneous actinide capture and release using functionalized carbon fiber electrodes (CF|CNT|^{PO}Cb and CF|CNT|^{PO}Cb-Pyr).

[a] *Department of Chemistry and Biochemistry, University of California, Santa Barbara, California 93106, USA.*
[b] *Department of Chemistry, University of Calgary, 2500 University Drive NW, Calgary, Alberta T2N 1N4, Canada. E-mail: gabriel.menard@ucalgary.ca*
Electronic Supplementary Information (ESI) available: synthesis, electrochemical details, spectroscopic details, ICP-OES data, XRD data. See DOI: 10.1039/x0xx00000x

other lanthanides and Cs, thus circumventing the need for biphasic extraction (Fig. 1b). While this was done in the context of SNF processing, this process could equally be envisioned for other applications, such as capturing uranyl from seawater.[6-12] To the best of our knowledge, this work is the first demonstration of grafting a molecular electrochemically switchable compound for selective capture and release of metals.

We started with the simplest approach to test the heterogeneous electrochemical behaviour of ^{PO}Cb by drop casting films using DCE solutions of ^{PO}Cb onto polished glassy carbon (GC) electrodes (GC|^{PO}Cb). While cyclic voltammograms (CVs) of the films in 0.1 M aqueous KCl showed no evident electrochemical response in the first scan, we observed quasi-reversible redox features grow in over 20 scans, with a formal reduction potential ($E_{1/2}$) of -0.55 V vs SCE (Fig. 2a). This value closely aligns with the solution state reduction potential of ^{PO}Cb in acetonitrile (-0.994 V vs $Fc^+|Fc$ ≅ -0.594 V vs SCE), upon accounting for the solvent and reference electrode used.[4, 13] In solution, ^{PO}Cb undergoes a chemically reversible 2 e^- reduction concurrent with C–C bond breaking to form the *nido* species, $^{PO}Cb^{2-}$, which can in turn undergo a 2e^- oxidation back to the *closo* species, ^{PO}Cb.[4] The observed redox events on GC|^{PO}Cb likely correspond to the heterogeneous analog given the observed potentials. The peak currents also remained relatively stable beyond 20 scans, with a linear dependence on the scan rate, indicative of a non-diffusional Faradaic response (i.e., pseudo-capacitance (Fig. S2)). These CVs demonstrate the GC|^{PO}Cb film is in ionic contact with the bulk aqueous solution – a surprising phenomenon considering the low polarity and hydrophobicity of *ortho*-carborane in general.[14-16]

We were interested in investigating if the addition of π-π stacking capability to our ^{PO}Cb would enhance the current density of the films. We thus synthesized 1,2-$(Ph_2PO)_2$-9-Pyrenyl-$C_2B_{10}H_9$ (^{PO}Cb-Pyr), which added a pyrene substituent to the back end of the carborane cage as a π-π stacking functional group (Fig 2b, inset). Films of ^{PO}Cb-Pyr on a GC electrode (GC|^{PO}Cb-Pyr) had similar electrochemical behaviour to the GC|^{PO}Cb films but with lower peak current densities and a higher peak-to-peak separation of 0.372 V compared to 0.195 V for the GC|^{PO}Cb films (Fig. 2a-b).

While both GC|^{PO}Cb and GC|^{PO}Cb-Pyr films were successfully generated on GC surfaces and subsequent *closo*↔ *nido* redox events were observed, it became clear from the observed current densities (μA/cm², Fig. 2a-b (y-axes)) that there was low surface coverage which would ultimately lead to a poor heterogeneous absorbent. To increase the areal density of ^{PO}Cb on the electrode, we added a layer of single walled carbon nanotubes (CNT) on the GC electrodes. This has been demonstrated with heterogeneous catalyst systems to reduce aggregation and increase dispersion of molecules on the surface, especially for catalysts containing π-π stacking functional groups, such as pyrene.[17, 18] Films were made by first drop casting CNT-in-DCE suspensions onto the surface of the GC electrode (GC|CNT).

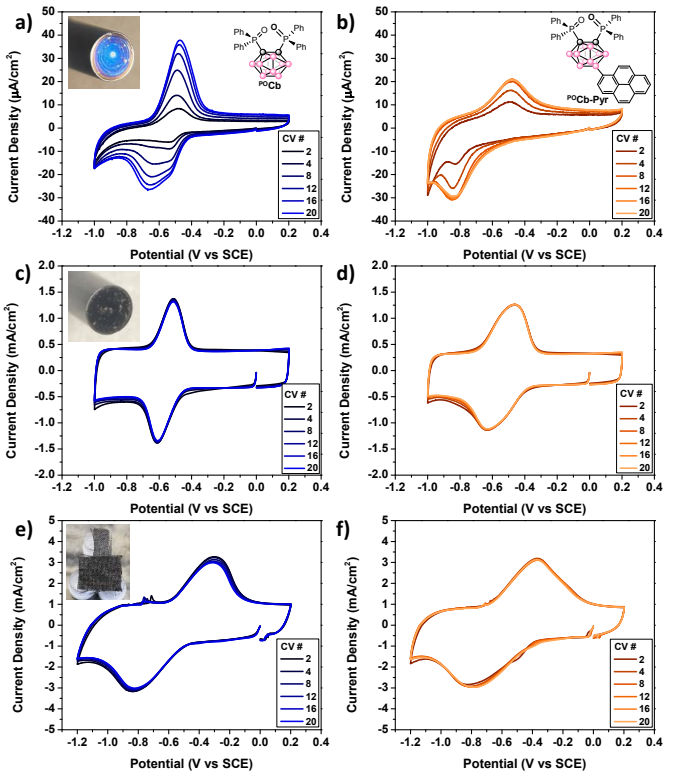

Fig. 2 Cyclic voltammograms of carborane films on glassy carbon rods and carbon fiber electrodes in 0.1 M KCl aqueous solutions at a scan rate of 0.1 V/s. a) GC|^{PO}Cb (inset picture of film). b) GC|^{PO}Cb-Pyr. c) GC|CNT|^{PO}Cb (inset picture of film). d) GC|CNT|^{PO}Cb-Pyr. e) CF|CNT|^{PO}Cb (inset picture of film). f) CF|CNT|^{PO}Cb-Pyr.

Next, ^{PO}Cb or ^{PO}Cb-Pyr in DCE was drop casted onto the GC|CNT to make the GC|CNT|^{PO}Cb and GC|CNT|^{PO}Cb-Pyr electrodes. Unlike the previous films, the GC|CNT|^{PO}Cb and GC|CNT|^{PO}Cb-Pyr films did not require conditioning CVs to facilitate the emergence of Faradaic current responses. Both the GC|CNT|^{PO}Cb and GC|CNT|^{PO}Cb-Pyr films saw significant increases in current densities (mA/cm² vs μA/cm²) and lower peak-to-peak separation (0.1 V and 0.174 V, respectively) compared to the non-CNT counter parts (Fig. 2c-d vs. 2a-b). Over the course of 20 CV scans, we noted the GC|CNT|^{PO}Cb-Pyr to be more stable than the GC|CNT|^{PO}Cb film which had a decay in peak current density of the oxidation and reduction that we attribute to the loss of ^{PO}Cb from the surface. We ascribe the higher stability of the GC|CNT|^{PO}Cb-Pyr film to the π-π stacking with the CNT in the GC|CNT|^{PO}Cb-Pyr film.

While the incorporation of CNT into the films resulted in significantly higher areal surface loadings of carborane, we next moved to still larger electrodes in order to measurably test UO_2^{2+} capture and release using ICP-OES. We employed carbon fiber cloth (CF) electrodes which were prepared in an analogous manner by drop casting CNT suspended in DCE to each side of a 4 cm² CF electrode (CF|CNT). To the CF|CNT, ^{PO}Cb or ^{PO}Cb-Pyr in DCE were drop casted onto each side of the electrodes (CF|CNT|^{PO}Cb, CF|CNT|^{PO}Cb-Pyr) (Fig. 2e, inset). Using CF electrodes approximately doubled the peak current densities relative to the GC|CNT systems, but also resulted in increased

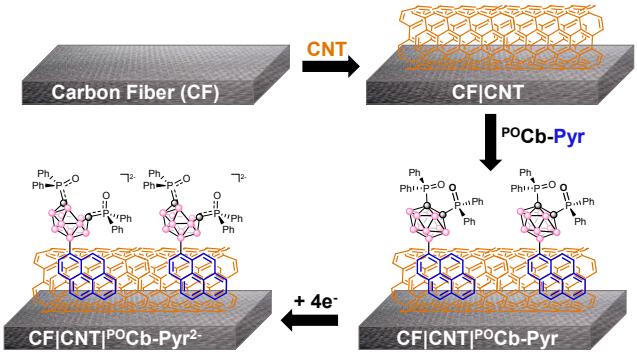

Fig. 3 Assembly and charging scheme of CF|CNT|^{PO}Cb-Pyr.

peak-to-peak separations (0.543 V and 0.425 V, respectively (Fig. 2e-f)). Similar to the GC|CNT|^{PO}Cb electrodes, the CF|CNT|^{PO}Cb electrodes revealed decreasing current densities over repeated scans, suggesting potential loss of ^{PO}Cb; this was not observed in the ^{PO}Cb-pyr electrodes, again suggesting strong π-π stacking. Together, these data suggest that CF|CNT electrodes offered a higher surface area due to the use of CF, while the CNT enhanced electrode stability and promoted ionic contact with aqueous solutions thus allowing significant generation of the *nido*-carboranes on the surfaces.

We scaled up the functionalized CF|CNT electrodes to 34 cm^2 to test their heterogeneous capture ability (Fig S5). These electrodes were galvanostatically reduced in an H-cell to generate the surface bound *nido*-carborane species (Fig. 3). The charged electrodes were then submerged in a stock solution containing equimolar $CsNO_3$, $Nd(NO_3)_3(THF)_3$, $Sm(NO_3)_3(H_2O)_6$, $Th(NO_3)_4(H_2O)_x$, and $UO_2(NO_3)_2(H_2O)_6$ in 0.1 M KCl for 10 minutes. The stock solution was subsequently drawn off the electrode and stored for analysis by ICP-OES. The electrodes were then brought outside the glove box and soaked in nitric acid overnight to oxidize the carborane and strip the captured metals into solution. CF|CNT, CF|CNT|^{PO}Cb, and CF|CNT|^{PO}Cb-Pyr electrodes not subjected to electrochemical reduction were also prepared as controls in order to deconvolute adsorption from electrochemical capture. All experiments were performed in triplicate with the stock solutions, captured solutions, and stripped (released) solutions being analysed by ICP-OES to determine metal concentrations.

Analysis of the CF|CNT control electrodes both with and without galvanostatic charging (gray bars and superimposed dashed bars, respectively; Fig. 4) revealed an average percent capture for the charged electrodes of 27.8% for Th^{4+} and 12.3% for UO_2^{2+}, both significantly higher than Cs^+, Nd^{3+} and Sm^{3+} each at ~ 3.7% capture. Most importantly, these values were within error of the uncharged CF|CNT electrodes indicating that galvanostatic charging of these controls played no role in metal adsorption. In contrast, comparing the charged carborane-tethered electrodes to the uncharged ones revealed stark differences. For instance, the charged CF|CNT|^{PO}Cb electrodes captured significantly higher quantities of the actinides, Th^{4+} (52.6 %) and UO_2^{2+} (31.7%), relative to ~5.4% capture of Cs^+, Nd^{3+}, and Sm^{3+} (Fig. 4, blue bars). Most importantly, these values were all significantly higher than both the uncharged CF|CNT|^{PO}Cb control (Fig. 4, superimposed dashed blue bars) and the CF|CNT controls (gray bars). The increase in percent capture shows that $^{PO}Cb^{2-}$, generated on the surface of the electrode, preferentially captures the actinides out of aqueous solution. Lastly, the charged CF|CNT|^{PO}Cb-Pyr electrodes were next analysed. Compared to CF|CNT|^{PO}Cb, here we observed a modest increase in the percent capture for Th^{4+} (66.1%) and UO_2^{2+} (53.1%); however, this also came at the expense of modestly higher capture rates of Cs^+, Nd^{3+}, and Sm^{3+} to ~12% each (Fig. 4, orange bars). The slightly higher extraction values of CF|CNT|^{PO}Cb-Pyr vs. CF|CNT|^{PO}Cb electrodes is likely due to the increased stability from the additional π-π stacking, which

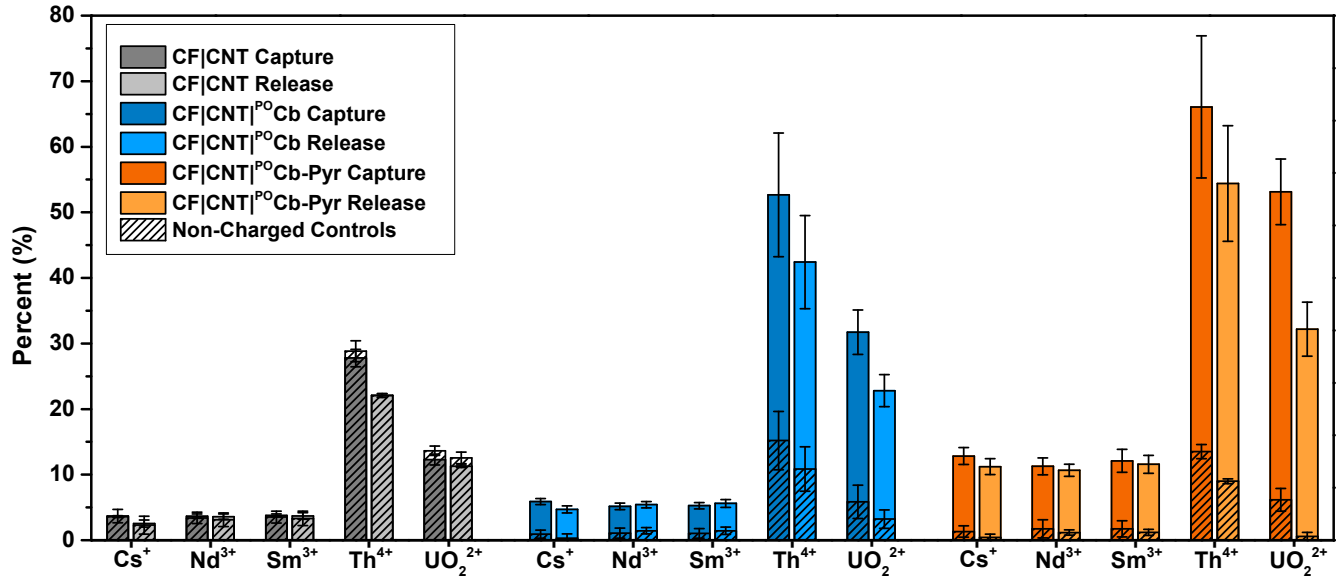

Fig. 4 Percent heterogeneous capture and release of selected metals from mixed metal aqueous solutions (Cs^+, Nd^{3+}, Sm^{3+}, Th^{4+}, UO_2^{2+}) performed in triplicate with charged and non-charged CF|CNT (gray), CF|CNT|^{PO}Cb (blue), and CF|CNT|^{PO}Cb-Pyr (orange) electrodes.

can help prevent the loss of ^{PO}Cb-Pyr^{2-} from the surface. In both cases, the uncharged CF|CNT|^{PO}Cb and CF|CNT|^{PO}Cb-Pyr electrodes showed significantly lower capture rates compared to the charged electrodes. This observation aligns with our biphasic work wherein the *closo* species, ^{PO}Cb, does not extract uranyl from aqueous solutions.[4, 5] In addition, we note that the CF|CNT|^{PO}Cb and CF|CNT|^{PO}Cb-Pyr capture controls (blue and orange dashed bars) are lower than in the CF|CNT controls. We attribute this to the surface-adsorbed carboranes blocking the non-specific binding sites on the surface of the CNTs. These results demonstrated that the CF|CNT preferentially binds the actinides over the alkali and lanthanides upon with the addition of ^{PO}Cb^{2-} and ^{PO}Cb-Pyr^{2-} to the surface significantly increasing the percent capture of actinides and the selectivity towards them.

Release of the captured metals could be easily performed by exposing the electrodes to 2% nitric acid in air, resulting in the oxidation of ^{PO}Cb^{2-}/^{PO}Cb-Pyr^{2-} to ^{PO}Cb/^{PO}Cb-Pyr and metal release. The percent released into a fresh solution followed the same trends as capture with the charged carborane-functionalized electrodes enriching the extracted solutions with the actinides (Th^{4+} and UO_2^{2+}). The CF|CNT|^{PO}Cb electrode was able to transfer 42.4% and 22.8% of the Th^{4+} and UO_2^{2+} present in the stock solution to a fresh solution (Fig. 4, pale blue bars). The CF|CNT|^{PO}Cb-Pyr was ~10% more efficient with 54.4% and 32.2% transferred Th^{4+} and UO_2^{2+}, respectively (Fig. 4, pale orange bars). This protocol provides an efficient and simple method to release the metals and enrich the actinides in the final solution over the alkali and lanthanide metals in a stock. Lastly, we note that recharging used functionalized electrodes rinsed with deionized water revealed charging plots consistent with unfunctionalized electrodes indicating likely loss of the carboranes from the surface upon oxidation with nitric acid. Current efforts are focusing on covalently binding the carboranes to electrode surfaces.

Conclusions

The results presented herein outline a facile adaptation of an electrochemically-driven solution-phase metal separation process into a heterogeneous process. Drop casted films of carborane complexes maintained ionic contact with aqueous solutions with stable pseudocapacitive electrochemical behaviour. We improved the heterogeneous electrodes via the addition of CNT to carbon surfaces, attaching pyrene anchoring groups to the ligand and using carbon fiber electrodes, culminating in CF|CNT|^{PO}Cb and CF|CNT|^{PO}Cb-Pyr electrodes with high yield capture and release of actinides selectively over lanthanides and alkali metals. Covalently binding carboranes to electrode surfaces and further tuning these systems for heterogeneous capture and release of UO_2^{2+} and other energy-important metals from seawater are currently being investigated.

Conflicts of interest

There are no conflicts to declare.

Acknowledgements

Arunavo Chakraborty is thanked for helpful discussions. We thank the National Science Foundation (CHE-2155239) and the Department of Energy, Office of Basic Energy Sciences (DE-SC0021649) for funding.

References

1. IAEA, Nuclear Power and the Paris Agreement, https://www.iaea.org/sites/default/files/16/11/np-parisagreement.pdf, Accessed 2/5/2021, 2021.
2. I. Kumari, B. V. R. Kumar and A. Khanna, *Nucl. Eng. Des.*, 2020, **358**, 110410.
3. J.-P. Glatz, in *Comprehensive Nuclear Materials (Second Edition)*, eds. R. J. M. Konings and R. E. Stoller, Elsevier, Oxford, 2020, pp. 305-326.
4. M. Keener, C. Hunt, T. G. Carroll, V. Kampel, R. Dobrovetsky, T. W. Hayton and G. Ménard, *Nature*, 2020, **577**, 652-655.
5. M. Keener, M. Mattejat, S.-L. Zheng, G. Wu, T. W. Hayton and G. Ménard, *Chem. Sci.*, 2022, **13**, 3369-3374.
6. C. W. Abney, R. T. Mayes, T. Saito and S. Dai, *Chem. Rev.*, 2017, **117**, 13935-14013.
7. M.-L. Feng, D. Sarma, X.-H. Qi, K.-Z. Du, X.-Y. Huang and M. G. Kanatzidis, *J. Am. Chem. Soc.*, 2016, **138**, 12578-12585.
8. Y. Song, C. Zhu, Q. Sun, B. Aguila, C. W. Abney, L. Wojtas and S. Ma, *ACS Cent. Sci.*, 2021, **7**, 1650-1656.
9. Z. Wang, R. Ma, Q. Meng, Y. Yang, X. Ma, X. Ruan, Y. Yuan and G. Zhu, *J. Am. Chem. Soc.*, 2021, **143**, 14523-14529.
10. Y. Yuan, Q. Meng, M. Faheem, Y. Yang, Z. Li, Z. Wang, D. Deng, F. Sun, H. He, Y. Huang, H. Sha and G. Zhu, *ACS Cent. Sci.*, 2019, **5**, 1432-1439.
11. F. Chi, S. Zhang, J. Wen, J. Xiong and S. Hu, *Ind. Eng. Chem. Res.*, 2018, **57**, 8078-8084.
12. C. Liu, P.-C. Hsu, J. Xie, J. Zhao, T. Wu, H. Wang, W. Liu, J. Zhang, S. Chu and Y. Cui, *Nat. Energy*, 2017, **2**, 17007.
13. D. Chang, T. Malinski, A. Ulman and K. M. Kadish, *Inorg. Chem.*, 1984, **23**, 817-824.
14. V. I. Bregadze, *Chem. Rev.*, 1992, **92**, 209-223.
15. S. Fujii, *Med. Chem. Commun.*, 2016, **7**, 1082-1092.
16. Y. Asawa, K. Nishida, K. Kawai, K. Domae, H. S. Ban, A. Kitazaki, H. Asami, J.-Y. Kohno, S. Okada, H. Tokuma, D. Sakano, S. Kume, M. Tanaka and H. Nakamura, *Bioconjugate Chem.*, 2021, **32**, 2377-2385.
17. N. Corbin, J. Zeng, K. Williams and K. Manthiram, *Nano Research*, 2019, **12**, 2093-2125.
18. L. Sun, V. Reddu, A. C. Fisher and X. Wang, *Energ. Environ. Sci.*, 2020, **13**, 374-403.